Future Journal of Pharmaceutical Sciences

RESEARCH

Open Access

In vitro and in vivo evaluation of crosslinked wound dressing loaded with combined rosuvastatin calcium and levofoxacin simultaneously determined by eco-friendly spectrophotometric method

Marwa A. Abd El-Fattah[1†], Asmaa O. El-Demerdash[2†], Heba A. Eassa[1,3*], Kamilia H. A. Mohammed[1], Israa A. Khalil[2], Asmaa H. Esmaeil[1], Shimaa E. Abdel Aziz[2] and Omnia M. Amin[1]

Abstract

Background Wound healing is a natural but complex process that can be delayed by infection. Rosuvastatin calcium (RVS) is an anti-hyperlipidemic that was recently reported to have a wound healing capability. The study aimed to investigate the impact of combining RVS with Levofloxacin (LV) on wound healing. A physically crosslinked polyvinyl alcohol (PVA) film loaded with RVS and LV was formulated as wound dressing. Formulation optimization was carried out using Box–Behnken design. The effect of independent variables (PVA and propylene glycol concentrations and the number of freeze–thaw cycles) on tensile strength (TS), elongation to break (%EB) and in vitro drugs' release was studied. For simultaneous RVS and LV quantification in the formulations and pure form, three spectrophotometric methods: derivative of ratio spectrophotometry, first derivative and mean centering, were developed. Also, their greenness was evaluated by the Analytical Eco-Scale and the Green Analytical Procedure Index. Then, the wound healing effect of the optimized wound dressing was evaluated in rat models.

Results The optimized dressing had sufficient mechanical strength (9.45 ± 0.67 MPa), adequate flexibility (112.6 ± 3.8% EB) and suitable drug release (52.3 ± 1.4% for LV and 38.99 ± 1.6% for RVS after 12 h). The proposed methods were validated following ICH guidelines, and greenness assessment suggested their very low environmental effect. The wound healing evaluation showed a higher wound contraction percentage when RVS was combined to LV. A histopathological study confirmed marked improvement in animals treated with combined formula with lowest inflammatory infiltration and optimum epithelialization, compared to other groups.

Conclusion Study findings suggest that combined LV-RVS dressing would be a beneficial platform with potentiated wound healing capacity.

Keywords Levofloxacin, Rosuvastatin, Wound dressing, Crosslinking, Derivative spectrophotometry

†Marwa A. Abd El-Fattah and Asmaa O. El-Demerdash have contributed equally to this work and are considered co-first authors.

*Correspondence:
Heba A. Eassa
heassa@usj.edu
Full list of author information is available at the end of the article

Graphic abstract

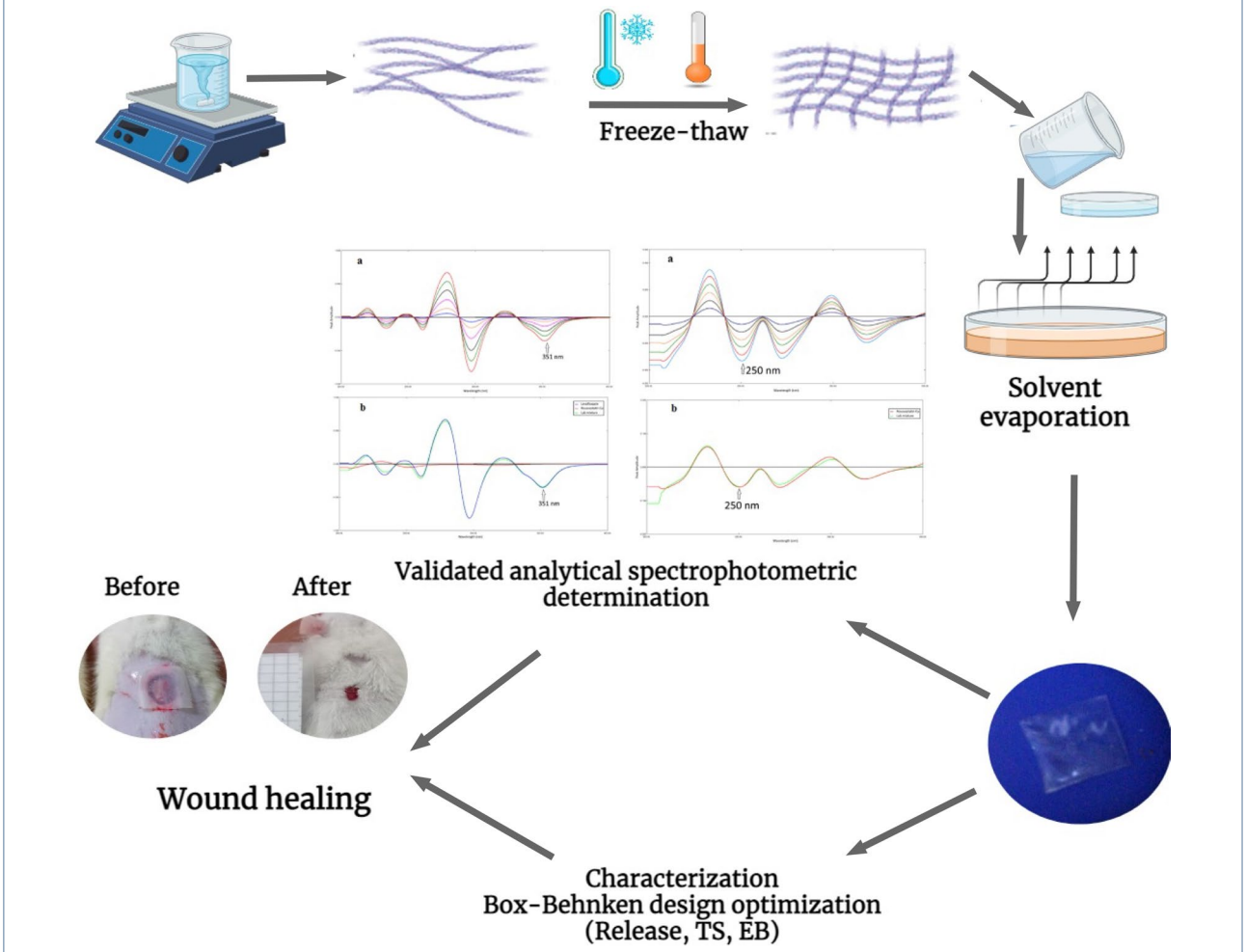

Background

Wounds, especially chronic ones, represent one of the greatest problems that significantly impact public health. Wound healing involves complex biological processes (inflammation, revascularization, hemostasis, proliferation and remodeling) to restore the normal structure and functions of the damaged skin which may extend to several months. Moreover, the susceptibility of wounds to infections with antibiotic-resistant bacteria could delay wound healing [1, 2]. Several wound healing modalities were used to promote/potentiate wound healing and to prevent bacterial infection. However, a need for more rapid wound healing together with adequate protection of the wound site from various infecting organisms is still required.

Levofloxacin (LV) is a slightly soluble broad-spectrum fluoroquinolone antibiotic with proven efficacy in the treatment of infected wounds [3, 4]. RVS is an antihyperlipidemic drug that gained attention for its wound healing ability. RVS reverses wound healing inhibitors such as farnesyl pyrophosphate (FPP) and potentiates vascular endothelial growth factor, an important step for new blood vessel production [5, 6]. Moreover, it has demonstrated an antimicrobial effect against *Staphylococcus aureus* through interference with bacterial protein synthesis [7]. It was reported that combining RVS with LV has a synergistic action against the microbial strains that commonly infiltrate infected wounds. Therefore, topical wound healing platforms containing both drugs would gain the merits of promoted tissue

regeneration by RVS, antibacterial property of not only LV but also the synergistic antibacterial effect of such combination [8, 9].

Polymeric films were utilized as dressing due to their ability to restore normal cellular function of damaged tissue [10, 11]. Film-based dressings offer many advantages, including the ability to maintain the proper moisture balance in the wound environment together with flexible properties that could be modified to match requirements for ideal wound healing [12]. PVA-based dressings were proposed in many studies. Crosslinking of PVA hydrogels can provide controlled drug release and enhanced mechanical properties. However, chemical crosslinking can be a source of impurities that would harm and infect open wounds. So, physical crosslinking would be a better alternative as a biocompatible, non-toxic eco-friendly method [9, 13, 14].

There are analytical techniques that have been proposed to determine each of RVS and LV including spectrophotometry [15, 16], colorimetry [17], fluorimetry [18] and electrochemical methods [19] In addition, chromatographic methods have also been reported for cited drug determination including HPLC [20, 21], TLC [22] and LC–mass spectrometry [23]. A comprehensive search of the literature revealed the lack of an analytical technique for the simultaneous determination of LV and RSV. Also, to our knowledge, a wound dressing formulation that combines both drugs has not been reported before. Hence, the present study is designed to investigate the impact of combining RVS with LV on wound healing along with developing a new analytical technique for the determination of RVS and LV in this new combination. Eco-friendly spectrophotometric methods are proposed for the simultaneous determination of both drugs in new wound dressing formulation. Moreover, the developed analytical approach is required as a means of evaluating the pharmaceutical properties of the dressing formulations. So, the spectrophotometric technique was specifically chosen due to its simplicity, short analysis time, cost-effectiveness and eco-friendliness. These are the most critical factors due to the large number of dissolution samples. Optimized dressing was designed using Box–Behnken design. The effect of formulation factors (PVA and PG concentrations and number of FT cycles) on TS, %EB and in vitro drugs released from the prepared wound dressings was investigated. Finally, optimized formulation was evaluated for wound healing in a rat model.

Methods

Materials

RVS was a kind gift from Egyptian International Pharmaceutical Industries Co. (Cairo, Egypt). LV was gifted by SEDICO Pharmaceutical Company (Cairo, Egypt), PVA was purchased from (Al Gomhoria Co, Egypt), and propylene glycol (PG) was obtained as a gift sample (EPICIO Co., Egypt). Methyl alcohol and dialysis bags (MW cut off of 12,000 Da) were purchased from Sigma Chemical Company (Sigma-Aldrich Corp., St. Louis, MO, USA).

Differential scanning calorimetry

To confirm compatibility between the drugs and between the drugs and the additives, thermal analysis was performed for each of RVS, LV, PVA and their physical mixture using a differential scanning calorimeter (DSC-60, Shimadzu, Japan) [24].

Formulation of PVA-based wound dressing

To obtain wound dressing with acceptable physicochemical properties and controlled drug release, the Box–Behnken statistical design was adopted using independent variables (% PVA (A), % PG (B) and number of FT cycles (C)). The levels of independent variables and the resultant constraints are listed in Table 1. Statistical analysis was performed using Design-Expert software (Design-Expert 11.1.0.1 Stat Ease Inc., Minneapolis, MN, USA). Different batches and their resulting responses are presented in Table 2.

PVA-based wound dressings were prepared by solvent casting method. In brief, PVA was first dissolved in 20 mL double distilled water at 90°C and stirred till clear, transparent solutions were obtained. The prepared solution was then cooled down to room temperature and the specified amount of PG was added and mixed. Required quantities of LV and RVS were separately dissolved in (5 mL) methanol under stirring and were slowly added to the prepared solution and stirred together till uniform mixing. The resultant mixture volumes were adjusted to 25 mL, then poured onto a glass mold and were further crosslinked by the application of different numbers of freeze–thaw cycles (Table 2). This was done by first freezing the mixtures for 16 h. at − 12 °C followed by thawing them for 8 h at room temperature. Finally, drying was performed at 30 °C for 48 h. The prepared wound dressings were packed in an aluminum foil and then stored in a desiccator [10, 13].

Eco-friendly UV spectrophotometric methods

For LV and RVS quantification, precise and sensitive spectrophotometric methods were used for the simultaneous estimation of both drugs in bulk powder and in the developed dressing formulation without prior separation.

Apparatus

A Shimadzu (UV-1601 PC) dual-beam UV–visible spectrophotometer, with 1cm quartz cells. Scans in the range of 200–400 nm were carried out with 0.2 nm intervals.

Table 1 Variables (independent and dependent) used in Box–Behnken design for the development and optimization of wound dressing

Variable	Levels		
	Low (− 1)	Medium (0)	High (+ 1)
PVA %	3	5.5	8
PG%	3	6	9
Freeze–thaw cycles (No.)	0	2	4
Dependent variables (Response)	**Constraints**		
R: Tensile strength (MPa)	Maximize		
R2: Elongation to break %	Maximize		
R3: LV release (12 h)	50%		
R4: RVS release (12 h)	50%		

Table 2 Box–Behnken design formulation codes and the observed responses

Run	Factor A: PVA (%)	Factor B: PG (%)	Factor C: FT* cycles	R1 TS** MPa	R2 EB*** (%)	R3 LV release 12 h (%)	R4 RVS release 12 h (%)
F1	3	3	2	6.3 ± 0.20	50.58 ± 1.2	64.38 ± 0.2	56.6 ± 1.0
F2	3	6	4	6.24 ± 0.10	62.35 ± 2.5	63.36 ± 2.1	52.2 ± 0.5
F3	5.5	6	2	6.76 ± 0.11	76.56 ± 3.4	52.47 ± 2.5	43.60 ± 2.2
F4	8	6	4	13.11 ± 0.32	51.25 ± 2.1	41.61 ± 1.1	29.03 ± 1.6
F5	8	6	0	10.65 ± 0.2	89.25 ± 3.4	47.76 ± 1.6	34.11 ± 0.4
F6	5.5	9	0	4.45 ± 0.10	110.05 ± 2.8	66.56 ± 0.2	54.38 ± 0.4
F7	5.5	3	0	6.98 ± 0.31	57.17 ± 1.0	58.60 ± 1.0	47.92 ± 0.6
F8	3	9	2	4.18 ± 0.10	103.36 ± 1.9	72.82 ± 0.2	60.75 ± 1.1
F9	5.5	9	4	6.22 ± 0.21	98.54 ± 2.3	57.06 ± 1.1	44.96 ± 0.4
F10	5.5	6	2	6.65 ± 0.21	74.4 ± 1.6	51.80 ± 1.6	44.80 ± 2.5
F11	8	9	2	9.97 ± 0.32	105.26 ± 2.7	47.18 ± 2.4	39.10 ± 1.5
F12	5.5	6	2	6.63 ± 0.22	73.0 ± 2.1	54.90 ± 2.1	41.10 ± 1.5
F13	5.5	6	2	6.54 ± 0.21	72.8 ± 1.4	49.70 ± 3.6	42.80 ± 2.3
F14	5.5	6	2	6.31 ± 0.16	73.4 ± 1.6	55.40 ± 1.9	44.50 ± 1.6
F15	8	3	2	14.1 ± 0.23	53.36 ± 0.8	37.81 ± 2.1	26.56 ± 1.8
F16	5.5	3	4	10.54 ± 0.14	44.18 ± 1.0	47.88 ± 1.6	39.36 ± 0.4
F17	3	6	0	4.33 ± 0.09	64.26 ± 1.3	73.31 ± 0.3	65.36 ± 1.3

Each dressing (2 × 2 cm) contained 50 mg LV and 10 mg RVS, *FT cycles: freeze–thaw cycles, **TS: tensile Strength, ***EB: elongation to break

Absorption and the derivative spectra of the proposed drugs were processed by Shimadzu UV-Probe version 2.32.

Procedure

i. Stock solutions of RVS and LV (1.0 mg/ mL) were prepared in pH 7.4 phosphate buffer. Working solutions of a concentration of 0.1 mg/mL from each drug were made by diluting the prepared stock solutions with phosphate buffer.

ii. Construction of calibration curves.

Aliquots of working solutions of RVS (50–300 µg) and LV (20–250 µg) in phosphate buffer were added in 10-ml volumetric flasks to be diluted with the buffer. The following procedure was repeated in triplicate. The solutions' spectra were scanned at 200–400 nm against phosphate buffer as a blank, saved in the computer and subjected to the following manipulations:

- Derivative ratio (DR) method for the simultaneous determination of RVS and LV: For RVS determination, the spectra of RVS were divided by the spec-

trum of (25 µg/ mL) of LV. Then ^{1}DR was obtained with scaling factor 10 and Δλ = 8 nm, and the ^{1}DR signal at 250 nm was measured. LV determination was obtained by dividing its spectra by RVS (30 µg/ mL) where ^{3}DR was created with scaling factor 100 and Δλ = 16 nm. The ^{3}DR signals at 295 nm and 261 were measured.

- First derivative (^{1}D) method for LV determination: ^{1}D spectra of the drug were created using scaling factor 10 and Δλ = 8 nm where its amplitude at 351 nm was measured for LV concentration.
- Mean centering method for LV determination: The zero-order spectra of the drug were divided by RVS (30µg/mL) and then mean-centered to calculate LV concentration at 346 nm.

iii. Different aliquot of RVS and LV

Mixtures containing different ratios of the two drugs were prepared by transferring different aliquots of RVS and LV working solutions into a set of 10-mL volumetric flasks and diluted with phosphate buffer. The drugs solutions were scanned, and their concentrations were calculated from the corresponding obtained regression equations.

iv. Application to pharmaceutical formulations

The developed wound dressings were dissolved in phosphate buffer and left on a magnetic stirrer for 15 min for complete dissolving. Then, the volume was completed to 300 mL with phosphate buffer and filtered to be used in the spectrophotometric methods. The filtrate, which is labeled to contain 0.0333 mg/ mL RVS and 0.1667 mg/ mL LV, was analyzed by the proposed methods after suitable dilution.

Effect of independent variables on mechanical properties of the developed dressing (TS and %EB)

TS was measured using Universal Materials Testing Machine Lloyd (Model LR 5K plus). Dressings (6 cm long × 2 cm wide) were subjected to pulling out at a speed of 20 mm/min with an applied load (5–35 N). TS and % EB were calculated using the equations [14, 25]:

$$\text{Ts (MPa)} = \left(\text{Breaking Force (N)}\right) / \left(\text{Cross} - \text{section area of Specimen} \left(\text{mm}^2\right)\right)$$

$$\%\text{EB} = \frac{(L2 - L1)}{L1} \times 100$$

where $L1$: initial length, $L2$: length after stretching (at the moment of rupture).

Measurements were carried out in triplicate, and the average was recorded.

Effect of independent variables on in vitro (LV and RVS) release

A wound dressing (2 cm × 2 cm) was placed in a dialysis bag which was then immersed into 300 mL of pH 7.4 phosphate buffer (simulating conditions of wound bed) solution maintained at 32°C and stirred at 100rpm using a shaking water bath (Gallen Kamp, England). Aliquots (5 mL) were withdrawn at certain time intervals and substituted immediately with equal volume fresh buffer. Amounts of LV and RVS were analyzed spectrophotometrically using the derivative ratio (DR) method after suitable dilution. The experiment was conducted in triplicate [26, 27].

Evaluation of wound dressing physical and water-related characters

Wound dressings were evaluated for uniformity of weight, pH and drug content [10, 28]. The content of LV and RVS was analyzed using the proposed established method. Results are presented as mean ± SD.

Folding endurance was recorded as the number of times the dressing could be folded (angle of 180°) at the same place without breaking or developing visible cracks [13].

The swelling index was calculated by placing accurately weighed dressing (2 cm × 2 cm) in 20 mL phosphate buffer pH 7.4 and reweighing dressings after specific time intervals after blotting with filter paper for removal of adhered moisture. The swelling degree (SI) was calculated by the following equation:

$$\%\text{SI} = \frac{(W_t - W_0)}{W_0} \times 100$$

where W_0 and W_t are observed weights for dressings before and after immersion in the medium, respectively[12].

Water vapor transmission rate (WVTR) was determined gravimetrically by placing the dressings tightly on the neck of a glass bottle containing saturated ammonium chloride solution (to provide an RH of 79.5%). The whole assembly was weighed and placed in a desiccator at 0% RH using anhydrous calcium sulfate at 25 °C. The assembly was reweighed at specific time intervals, and WVTR was calculated from the following equations [29];

$$\text{WVTR} = \frac{\Delta m}{\text{Dressing area}}$$

where Δm is the weight difference between two weight measurements.

Data analysis of Box–Behnken model

Different polynomial models were generated for the obtained responses. The effect of each variable was identified based on the resultant coefficients of interactions. Analysis of variance (ANOVA) was performed to study the statistical validity of the model. Response surface plots were generated utilizing Design-Expert software. The desirability function was used to determine the optimum formulation, which was then prepared and evaluated for subsequent comparison to predicted responses.

Wound healing evaluation of the optimized formulation

Wound healing efficacy was studied using Wister rats, weighing 150 ± 20 g. For one week before the study, animals were housed in individual cages at controlled temperature (25 °C ± 0.5) and humidity (RH of 60 ± 5%) at 12-h dark/light with free access to food and water. The animal was handled following a protocol approved by the ethics committee, (NUB-410–23).

Wounds were created under the condition of stable anesthesia (ketamine (100 mg/kg) / xylazine (10 mg/kg)). The back of the rat (the dorsal area between the shoulder blades) was shaved followed by cleansing the surgical site with ethanol swap. Full-thickness, excision wounds (18 mm) were made. Four groups were used for the study (six animals per group). Group 1 received LV containing wound dressing, while Group 2 received RVS containing wound dressing. Group 3 received RVS and LV containing wound dressing. The dressings were changed daily up to 12 days. Group 4 received normal saline (control). Percent wound contraction was calculated on days 0, 4, 7 and 12 using the following equation [30, 31].

$$\%\ \text{of wound contraction} = \frac{\text{wound area in day (zero)} - \text{wound area in day } (n)}{\text{wound area in day (zero)}} \times 100$$

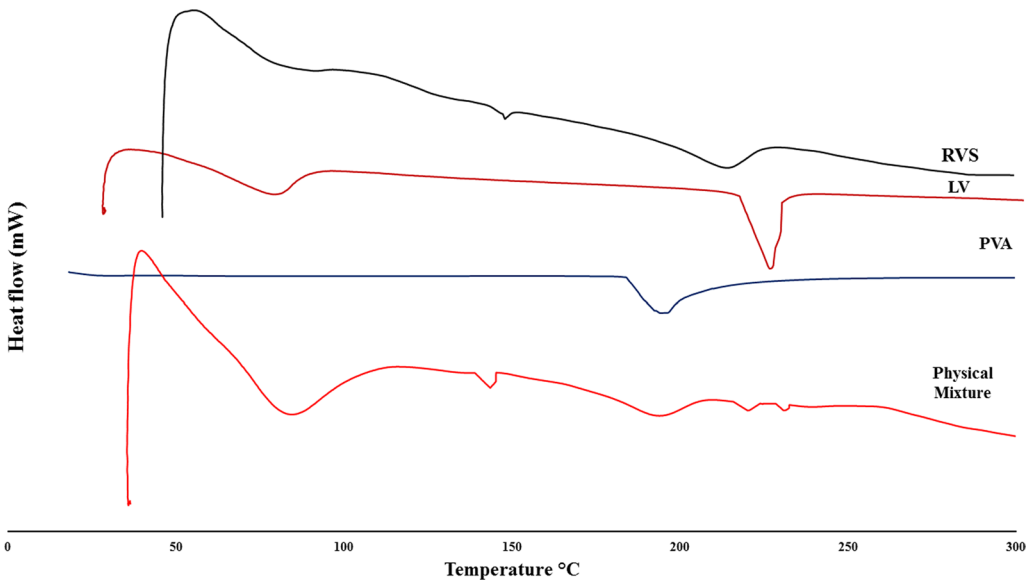

Fig. 1 DSC thermograms of RVS, LV, PVA and their physical mixtures

On the last treatment day, animals were killed, and skin sections (1 cm^2) for wound areas were collected and fixed in formaldehyde (10%) for histological study. Samples were frozen and cut transversely from the middle region of the wounds into sections (5-µm-thickness). Sections were then stained with Hematoxylin and eosin prior to examination using a light microscope. Samples were examined for epithelization, fibrosis as well as appearance of hair follicles [31–33].

Results

Differential Scanning Calorimetry

DSC thermograms of LV, RVS, PVA and their physical mixture are displayed in Fig. 1. Thermogram of LV presented a broad endothermic peak at about 80 °C and another sharp endothermic peak at about 230 °C corresponding to its melting [34]. RVS presented two peaks observed at 150 and 220 °C due to its semi-crystalline nature [35, 36]. These peaks appeared almost unchanged in the thermogram of the physical mixture. The additional peak at 195 °C could be attributed to PVA [37].

UV spectrophotometric method

UV spectra of both drugs showed severe overlap; a usual drawback in spectrophotometric analysis (Supplementary Fig. 1). LV spectrum had more sensitive and strong absorption bands which made separation of RVS more difficult. Several methods were tried to overcome this problem.

Derivative ratio method (DR)

This method involves the division of the mixture spectrum by the spectrum of one component (divisor) to create the derivative spectrum of the other component. The calculated derivative spectrum will be independent on the divisor, so it can be determined without interference [38]. The selection of divisors is of particular importance to get low noise and high sensitivity.

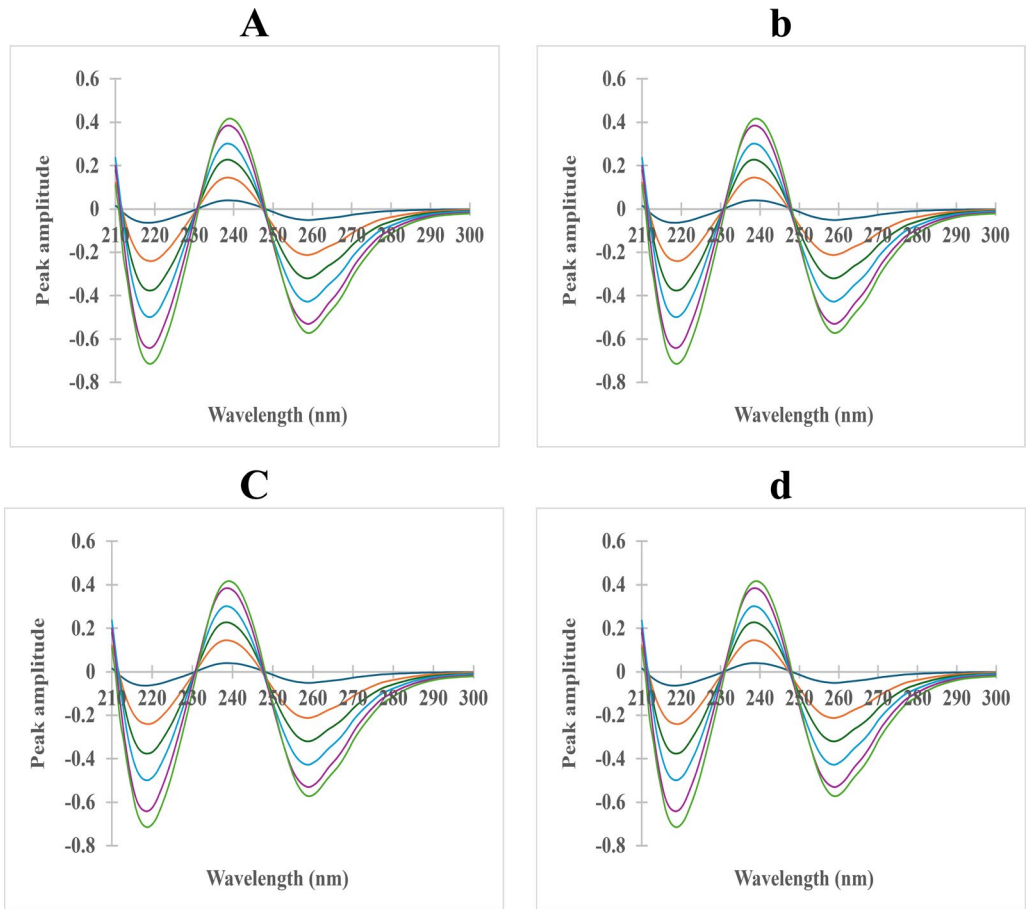

Fig. 2 Proposed spectrophotometric methods for simultaneous RVS and LV quantification in phosphate buffer. **a** First DR spectra of RVS (5–30 µg/mL) using LV 25 µg/mL as a devisor at 250 nm. **b** Third DR spectra of LV (2–25 µg/mL) using RVS 30 µg/mL as a divisor at 268 and 295 nm. **c** First D spectra of LV (2–25 µg/mL) at 351 nm in phosphate buffer. **d** Mean-centered ratio spectra of LV using RVS 30 µg/mL as a divisor at 364 nm

Different concentrations of RVS (2, 15 and 30 µg/mL) and LV (2, 10 and 25 µg/mL) divisors were tested before developing the method. The concentrations of 30 µg/mL of RVS and 25 µg/mL of LV were the selected divisors regarding low noise and maximum sensitivity.

The derivative orders of the ratio spectra (1st, 2nd, 3rd and 4th) were also tried to attain the best wavelength interval. Besides, different Delta λ values were tested (2, 4, 8 and 16) as they affect the shape, intensity and position of peaks of the analyzed drug. In addition, a scaling factor was attempted. The first derivative ratio (^{1}DR) was the most effective for RVS determination with scaling factor 10 and Δλ = 8 nm, while the third derivative ratio (^{3}DR) was created with scaling factor 100 and Δλ = 16 to measure LV. The wavelength choice was tested as well, where the amplitudes at 250 nm for RVS (Fig. 2a), and 268 nm and 295 nm for LV (Fig. 2b) showed optimum recovery percentages in laboratory-prepared mixture.

First derivative

The first derivative (^{1}D) spectrum (Fig. 2c) showed zero crossing points of the RVS only at 351 nm at which LV was determined. Different Δλ values were tried (2, 4, 8 and 16), where Δλ = 8 nm and scaling factor = 10 provide maximum peak heights with minimum noise.

Mean centering method (MNCN)

Basically, it is a simple method involving dividing the target analyte by the interfering components, then mean centering the ratio spectra resulted using MATLAB software [39]. The zero-order absorption spectra of LV were divided by RVS (30 µg/mL). The attained ratio spectra were mean-centered where the peak amplitudes were recorded at 346 nm (Fig. 2d).

Validation of method as per ICH recommendation

Linearity: The linearity range was 5–30 µg/mL for RVS and 2–25 µg/mL for LV. Regression parameters were calculated (Table 3).

Accuracy: The standard addition technique was used to check the accuracy. Both drug concentrations were obtained from the corresponding regression equations, and percentage recoveries revealed good accuracy of the established methods (Table 3).

Precision: It was calculated using 3 concentrations of each of RVS (5, 20, 30 µg/mL) and LV (2, 10, 25 µg/mL). Samples were analyzed three times on the same day (Repeatability) and three successive days (interday) by the proposed methods. Table 3 shows that the values of the RSD are acceptable.

Table 3 Regression, assay validation and statistical parameters for RVS and LV spectrophotometric determination

Regression parameter	RVS		LV				
	^{1}DR	Reported method [15]	^{3}DR		^{1}D	MNCN	Reported method [16]
λ max (nm)	250	244	268	295	351	346	298
Linearity range (µg/ mL)	5–30	2–18	2–25				3–8
Slope ± S.D	0.0110 ± 0.0001	–	0.0062 ± 4.07e^{-05}	0.0156 ± 0.0001	0.014 ± 8.60943 e^{-05}	0.9707 ± 0.0045	–
Intercept ± S.D	0.0047 ± 0.0021	–	0.0004 ± 0.0005	0.0005 ± 0.0015	0.0009 ± 0.0011	− 0.0749 ± 0.0680	–
S.D. of residual	0.0031	–	0.0009	0.0026	0.0020	0.0887	–
R^2	0.9994	–	0.9997	0.9996	0.9998	0.9998	–
Accuracy (mean% ± SD)	101.33 ± 0.67	–	99.64 ± 1.60	101.09 ± 0.68	99.92 ± 1.17	100.43 ± 0.60	–
Precision (RSD%)							
Intraday	0.27–0.43		0.18–0.94	0.30–1.71	0.16–0.77	0.31–1.01	
Interday	0.33–0.87	–	0.29–1.95	0.26–1.03	0.16–0.85	0.10–1.83	–
Statistical parameters							
N	5	5	5				5
Mean %	98.98	98.66	99.12	100.53	100.50	100.15	100.86
S.D	1.12	0.97	1.68	1.62	1.48	0.36	0.76
Variance	1.26	0.93	2.84	2.61	2.20	0.13	0.57
t test* (2.31)	0.49	–	1.35	0.41	0.49	1.91	–
F test* (6.39)	1.35	–	0.20	4.59	3.86	0.22	–
Standard addition Mean% ± S.D	101.33 ± 0.67	–	99.64 ± 1.60	101.09 ± 0.68	99.92 ± 1.17	100.43 ± 0.60	–

*Figures in parenthesis are the theoretical values of t and F at p = 0.05

Selectivity: The proposed methods' selectivity was achieved by the analysis of different laboratory-prepared mixtures of RVS and LV. Simultaneous determination of the two drugs was achieved without any interference (Supplementary Figs. 2 and 3). Thus, the established methods were proved to be selective as indicated by acceptable recovery results ranging from 98.55 to 101.25 (Supplementary Table 1).

Based on the previous findings, the developed methods were successfully carried out for the simultaneous determination of RVS and LV in their new combined topical preparation without preliminary separation. The derivative ratio (DR) method was the only selected technique for monitoring the two studied drugs in the dissolution study because ^{1}DR was the only effective one for RVS determination.

Evaluation of greenness of UV spectrophotometric method

Green analytical chemistry is a concept of promoting the utilization of energy-efficient instruments, reducing the consumption of toxic compounds and minimizing waste production in analytical procedures. Hence, this approach is well-regarded and commonly applied in analytical chemistry laboratories [40].

In this work, we used two common and complementary methods for evaluating the greenness of analytical techniques to assess the proposed spectrophotometric method, namely The Analytical Eco-Scale and GAPI. The Analytical Eco-Scale is a quantitative method that subtracts penalty points out of 100 points. It evaluates various factors, including the quantity and hazard level of reagents, energy consumption, occupational hazards and the amount of waste generated [41]. As shown in Table 4, the proposed technique scored 92 and outperforms the two previously reported spectrophotometric methods [15, 16]. The second method for the assessment of the greenness is GAPI. It is a color code evaluation of each stage. The red color symbolizes indicates high environmental impact. Yellow and green colors represent medium and low impacts [42]. GAPI tool shows that our proposed method has a higher level of greenness in comparison to the two reported methods (Fig. 3).

Tensile strength

The developed dressings had TS values (4.18 ± 0.1–14.1 ± 0.23 MPa) (Table 2). The quadratic model was the best as indicated by the highest regression coefficient value. The model's significance was assessed by $P < 0.001$. The quadratic model had a predicted R^2 (0.9781) close to the adjusted R^2 (0.9952) (Supplementary Tables 2 and 6) indicating a good correlation. The developed equation's fitting degree is considered fine as indicated by a non-significant lack of Fit; F value of 2.10. Figure 4a–c shows the response surface plots drawn by Design-Expert. The final equation developed based on data analysis for prediction of the response was:

$$\begin{aligned}\text{TS (MPa)} = {} & 6.58 + 3.35A - 1.64B + 1.21C - 0.5025AB \\ & + 0.1375AC - 0.4475BC + 1.80A^2 + 0.2622B^2 - 0.2073C^2\end{aligned}$$

Table 4 Penalty points of the proposed methods according to the Analytical Eco-Scale

Penalty points	Proposed UV spectrophotometry	Reported UV spectrophotometry for RSV [15]	Reported UV spectrophotometry for LV [16]
Reagents score			
Phosphate buffer	3	–	–
Methanol	–	6	6
Instruments score			
Energy	0	0	0
Occupational hazards	0	0	0
Waste	5	5	5
Total Penalty Points	∑ 8	∑ 11	∑ 11
Analytical Eco-Scale total score	92 Excellent green analysis	89 Excellent green Analysis	89 Excellent green Analysis

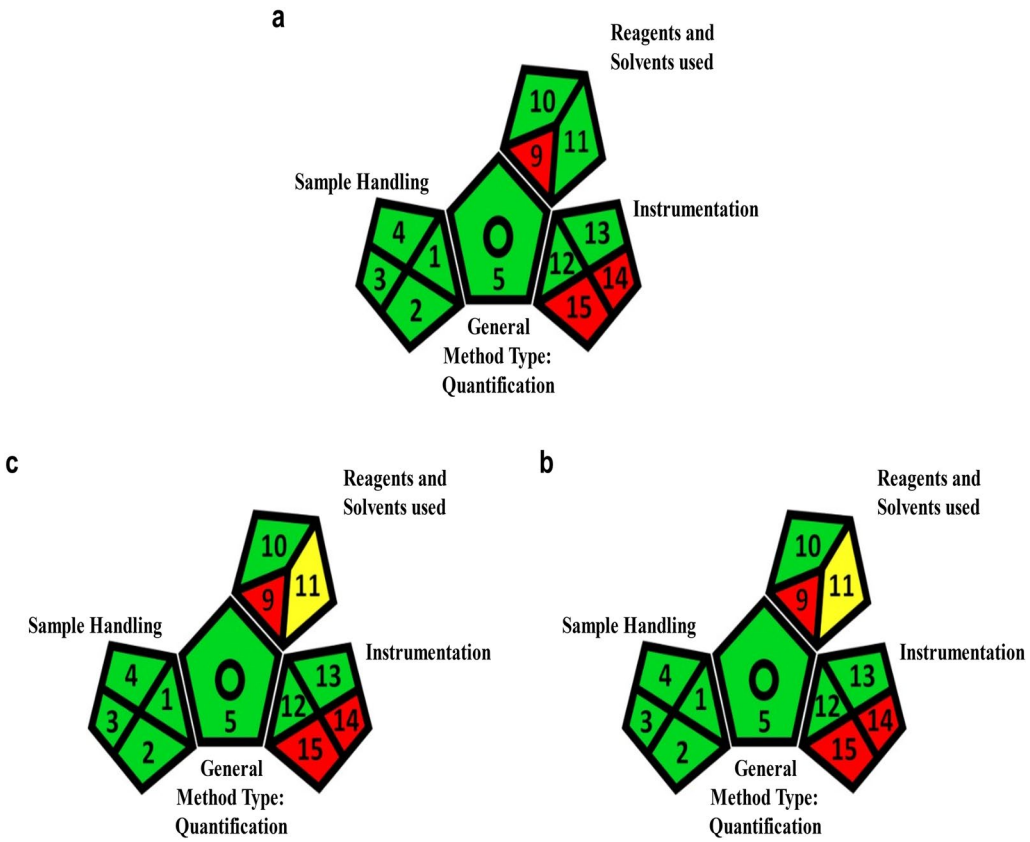

Fig. 3 GAPI approach for greenness assessment of: **a** the developed UV spectrophotometric methods, **b** the reported UV spectrophotometric method for RVS [15], **c** the reported UV spectrophotometric method for LV [16]

Elongation to break (%EB)

The developed dressings %EB values ranged from 44.18 ± 1.0 to 110.05 ± 2.8% (Table 2). The high coefficient value indicates that the quadratic model was the best model with high significance ($P < 0.001$). Its predicted R^2 (0.9022) was close to the adjusted R^2 (0.9832) (Supplementary Tables 3 and 6) indicating a good correlation. Non-significant lack of fit F value of 5.76 reveals the fine degree of fitting for the developed equation. Figure 4d–f shows the response surface plots drawn by Design-Expert. The final equation developed was:

$$\% \ \text{EB} = 74.03 + 2.32A + 26.49B - 8.05C - 0.2200AB - 9.02AC + 0.3700BC - 3.30A^2 + 7.41B^2 - 3.95C^2$$

In vitro drug release

Results for LV and RVS release (Table 2 and Fig. 5) showed the lowest release (37.81, 26.66% for LV and RVS, respectively) at 12th h for F15, while F17 showed the highest release at the same time (73.31 and 65.36% for LV and RVS, respectively).

Box–Behnken statistical analysis confirmed the suitability of the quadratic model as illustrated by regression coefficient value. The model was significant ($P < 0.001$) (Supplementary Tables 3 and 4). The predicted R^2 (0.9286 and 0.9590 for LV and RVS, respectively) were close to adjusted R^2 (0.9623, 0.9837 for LV and RVS, respectively) (Supplementary Tables 5 and 6) indicating good

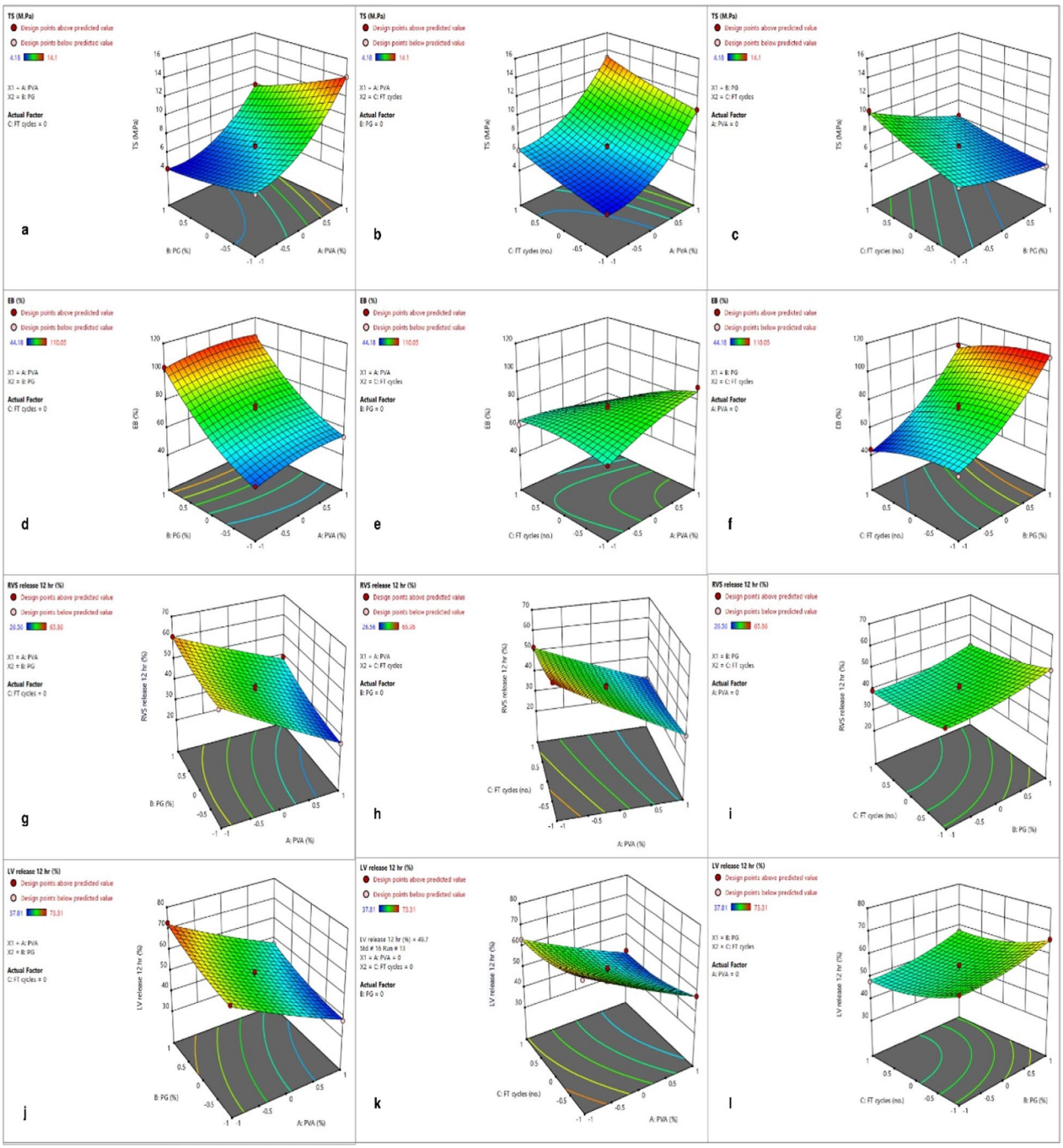

Fig. 4 Response surface plot illustrating the effect of variables on TS (MPa), %EB and in vitro drugs release **a** % PVA and % PG **b** % PVA and number of FT cycles and **c** % BG and number of FT cycles on TS (MPa) (R1) of the prepared dressings, **d** %PVA and %PG **e** % PVA and number of FT cycles and **f** % BG and number of FT cycles on EB (R2) of the prepared dressings, **g** % PVA and % PG **h** % PVA and number of FT cycles and **i** % PG and number of FT cycles on LV release (R3) of the prepared dressings, **j** % PVA and % PG **k** % PVA and no of FT cycles and **l** % PG and number of FT cycles on RVS release (R4) of the prepared dressings

correlation. Non-significant lack of fit F values (0.3164 and 0.5452 for LV and RVS, respectively) suggest a fine degree of fitting for the developed equations. Figure 4h–i shows the response surface plots drawn by Design-Expert. The final equations for predicting the responses were:

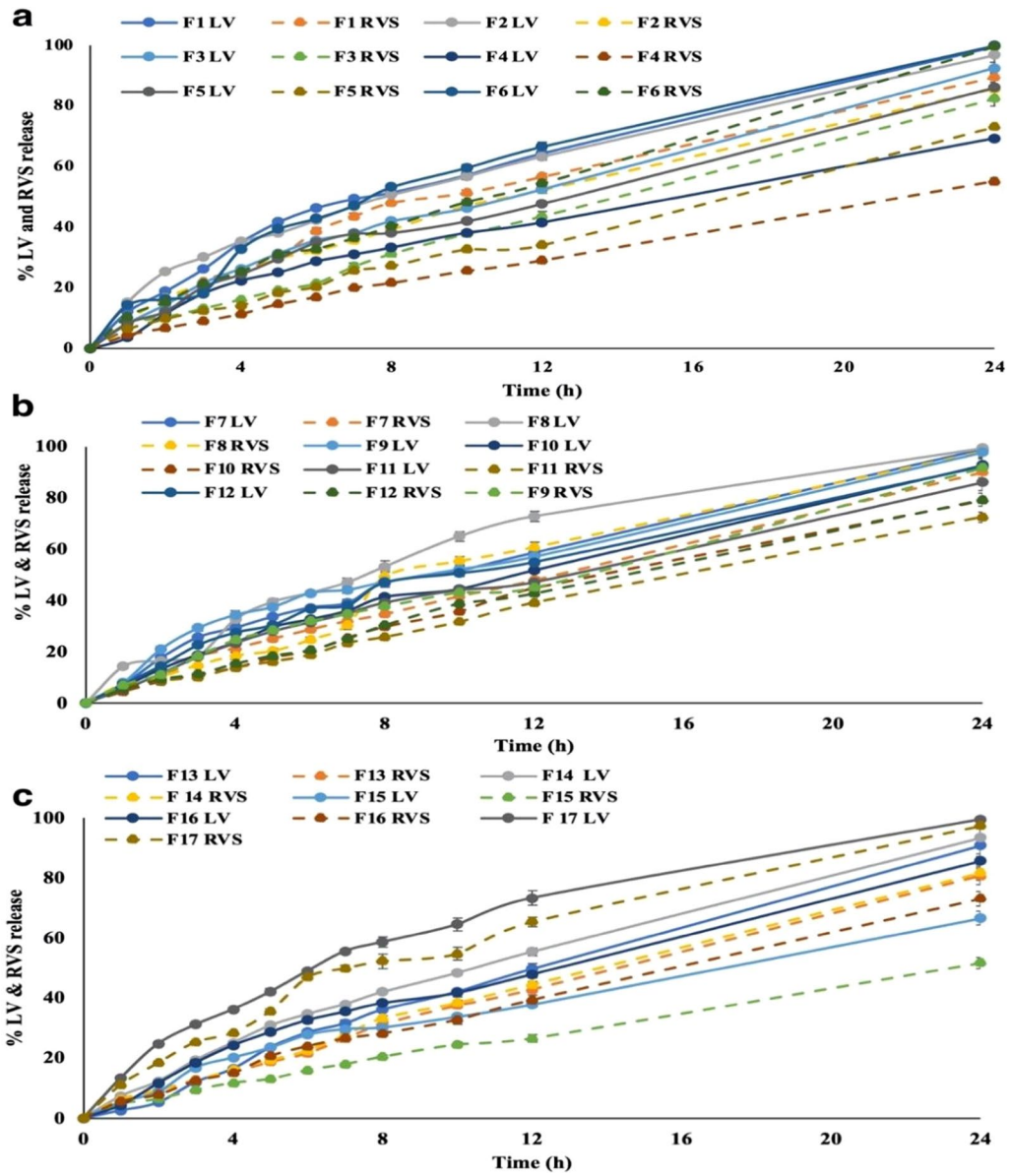

Fig. 5 Cumulative LV (–-) and RVS (---) release from wound dressings. **a** F1–F6, **b** F7–F12, **c** F13–F17

$$\text{LV release after 12 h} = 52.85 - 12.44A + 4.37B - 4.54C + 0.2325AB + 0.9500AC + 0.3050BC + 0.8392A^2 + 1.85B^2 + 2.82C^2$$

$$\text{RVS release after 12 h} = 43.36 - 13.26A + 3.59B - 4.53C + 2.10AB + 2.02AC - 0.2150BC + 0.4562A^2 + 1.94B^2 + 1.36C^2$$

Table 5 Evaluation of wound dressing physical and water-related characteristics

Run	Weight (mg)	pH	LV content (%)	RVS content (%)	Folding (no of folds)	SI (% after 3 h)	WVTR* (g/m^2/day)
F1	320 ± 15	6.5 ± 0.30	98.45 ± 0.22	98.85 ± 0.30	276 ± 12	SI (%)	2199.89 ± 35.2
F2	330 ± 12	6.2 ± 0.25	97.45 ± 0.55	96.98 ± 0.90	> 300	135.8 ± 5.3	2235.67 ± 23.1
F3	370 ± 25	6.3 ± 0.10	96.50 ± 0.93	97.56 ± 0.21	> 300	121.6 ± 4.6	2325.09 ± 32.6
F4	420 ± 26	6.5 ± 0.12	97.22 ± 0.31	98.52 ± 0.12	> 300	170.4 ± 9.8	1967.39 ± 30.6
F5	430 ± 22	6.5 ± 0.20	96.97 ± 0.81	97.42 ± 0.11	264 ± 19	188.8 ± 11.6	2289.33 ± 41.3
F6	380 ± 25	6.4 ± 0.11	97.54 ± 0.30	96.98 ± 0.98	> 300	196 ± 12.1	2629.15 ± 36.5
F7	380 ± 32	6.3 ± 0.09	97.01 ± 0.98	98.02 ± 0.87	> 300	190.3 ± 11.2	2325.09 ± 25.9
F8	330 ± 15	6.7 ± 0.14	96.54 ± 0.13	98.56 ± 0.35	> 300	150 ± 10.5	2450.29 ± 34.6
F9	380 ± 28	6.4 ± 0.10	97.32 ± 0.13	97.89 ± 0.22	> 300	129.6 ± 6.1	2365.98 ± 26.3
F10	371 ± 26	6.4 ± 0.20	97.06 ± 0.31	98.08 ± 0.45	> 300	181.2 ± 8.6	2244.75 ± 48.2
F11	440 ± 33	6.3 ± 0.15	97.87 ± 0.19	99.15 ± 0.98	296 ± 14	170.1 ± 5.3	2199.89 ± 22.1
F12	369 ± 40	6.3 ± 0.13	96.89 ± 0.21	98.50 ± 0.80	> 300	214.1 ± 12.6	2221.26 ± 26.5
F13	372 ± 25	6.4 ± 0.21	97.05 ± 0.81	97.88 ± 0.50	> 300	170.9 ± 8.6	2239.36 ± 12.6
F14	370 ± 24	6.5 ± 0.22	98.05 ± 0.41	97.65 ± 0.18	> 300	165.8 ± 5.3	2251.11 ± 26.6
F15	420 ± 34	6.4 ± 0.13	98.20 ± 0.81	99.21 ± 0.36	> 300	162.7 ± 8.7	2199.89 ± 26.9
F16	380 ± 25	6.4 ± 0.16	97.65 ± 0.25	97.25 ± 0.95	> 300	185.6 ± 12.3	2235.67 ± 37.8
F17	350 ± 24	6.6 ± 0.24	97.88 ± 0.61	98.44 ± 0.58	> 300	147.1 ± 8.6	2325.09 ± 43.2

WVTR water vapor transmission rate, *SI* swelling index

Evaluation of wound dressing physical and water-related characters

The formulated wound dressings had average weight and pH values of 320 ± 15–440 ± 33 mg and from 6.2 ± 0.25 to 6.7 ± 0.14, respectively (Table 5). Drug content was in the range of 96.50 ± 0.93–98.45 ± 0.22% for LV and 96.98 ± 0.98–99.21 ± 0.36% for RVS (Table 5). Folding endurance ranged from 264 ± 19 to > 300 (Table 5).

A swelling study showed increasing SI up to the maximum, followed by an equilibrium (no further water absorption) (Supplementary Fig. 4).

WVTR values of the prepared dressings ranged from 1967.39 ± 30.6 to 2629.15 ± 36.5 g/m^2/day (Table 5).

Optimization of wound dressing formulations

The mechanical property is important to ensure optimum physical protection of the wound by the applied dressing. Sufficient mechanical properties are also needed to support cellular processes including proliferation, tissue remodeling and angiogenesis. For %EB, dressings also needed to be flexible, soft and elastic to adapt to different body parts. Percent elongation to break was measured as an indicator of the dressing's extendibility from its initial length up to its break (extendibility) [29, 43]. Hence, optimum values for TS (MPa) and %EB were set to maximize TS and %EB to ensure dressing durability and flexibility in the applied area.

Dressings are generally designed to be replaced every 1–3 days [10, 44]. The current study aimed to ensure dressings provide controlled drug release for 24 h while maintaining dressing integrity. So, an optimum value for LV and RVS release at 12th h was set to 50% to ensure controlled drug release for 24 h.

Optimum formulation with 0.741 desirability was identified using Design-Expert software and was formulated using 8% PVA, and 9%PG and subjected to one FT cycle. Optimized formulation showed predicted values of 9.542 MPa for TS, 113.975 for %EB with about 50.00, 39.84% LV and RVS release, respectively. Experimental values were 9.45 ± 0.67 MPa for TS, 112.6 ± 3.8 for %EB and 52.3 ± 1.4, 38.99 ± 1.6% for LV and RVS release, respectively.

Wound healing evaluation

Time-dependent progression in wound contraction percent was observed in tested groups (Fig. 6a and b). The normal healing process was observed in the control group which exhibited only slight wound contraction percent (11.57 ± 1.13, 25.93 ± 4.54and 56.94 ± 2.32% after 4, 7 and 12 days, respectively). Group 1 (treated with LV-wound dressing) showed wound contraction percentages of 17.12 ± 2.73, 50.46 ± 1.13 and 71.75 ± 3.24% after 4, 7 and 12 days, respectively. For group 2 (RVS wound dressing), contraction percentages were 21.75 ± 3.69, 43.05 ± 3.4 and 68. ± 2.32% after 4, 7 and 12 days, respectively. Group 3 (LV/RVS wound dressing) showed significantly ($p < 0.001$) higher wound contraction percent

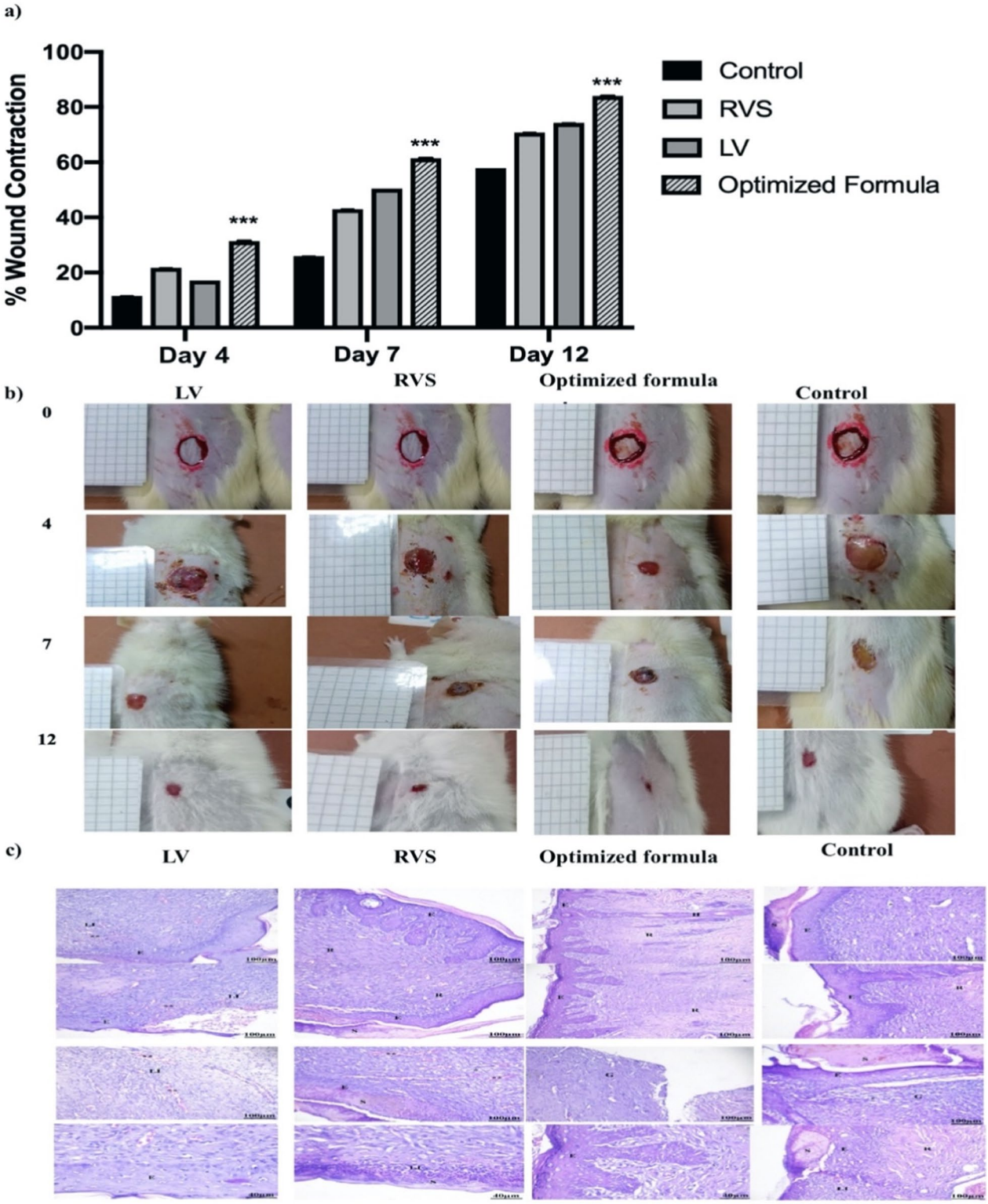

Fig. 6 Wound healing study in rat model. **a** Percentage wound contraction, **b** photographs wound healing phases and **c** histopathology in control group and in groups receiving LV, RVS, LV + RVS wound dressings (inflammation (LI), edema (*) and congestion (**), regenerated epithelium (E), reticular layer (R), scab development (S) and hair follicle (H)

compared to other groups (32.4 ± 2.27, 61.5 ± 1.85 and 84.3 ± 1.98% after 4, 7 and 12 days, respectively).

Histopathological examination (Fig. 6c) provides evidence for wound healing progression. Histopathological evaluation of the control group showed that the wound area had significant inflammation (LI), considerable edema (*) and marked congestion (**). The epithelium was only partially regenerated (E) in some wound areas with a partial development of the reticular layer (R). Scab development (S) was highly observed in the wound area.

In animals treated with LV-wound dressing, tissue sections showed a high degree of inflammation (LI), moderate edema (*) and minor congestion. Epithelium was partially restored (E). Animals treated with RVS wound dressing showed wound areas with moderate inflammation (LI), considerable edema (*) and congestion (**) in the newly formed tissues. There were areas for fully regenerated epithelium (E) and some areas of organized reticular layer (R) indicating RVS wound healing ability. In animals treated with RVS/LV-wound dressing, tissue sections showed a lower degree of inflammation (LI) and congestion (**). Granulation tissue formation was observed indicating a successful re-epithelialization process. The epithelium was well developed with some areas containing hair follicles (H).

Discussion

The study employed various spectrophotometric techniques to quantify RVS and LV simultaneously in a phosphate buffer solution. The derivative ratio spectrophotometry (DR) proved to be effective in separating the RVS and LV simultaneously. RVS was measured using a ^{1}DR at a wavelength of 250 nm, while the LV was determined using a ^{3}DR at wavelengths of 268 nm onwards. In addition, the first derivative (^{1}D) and the mean centering methods were successfully employed to determine the LV in the presence of RSV at measurements of 351 and 346 nm, respectively. Satisfactory results indicate that both drugs can be simultaneously determined by the developed methods with no interference from excipients and additives (Table 3). It is noteworthy that the development of a green and inexpensive analytical method is required as a tool for evaluating the properties of the new wound dressing formulation. The pharmaceutical properties of this wound dressing such as drugs' release and content were evaluated by the developed spectrophotometric method.

Compared to the previously reported methods which are a direct UV measurement of either LV or RSV alone in its formulations [15, 16], the suggested methods showed no considerable differences concerning accuracy and precision (Table 3). Moreover, the developed methods were considered more selective than the reported ones. Because of the quantitative estimation of RVS and LV in their new combined formulations could be performed successfully without any separation. Also, the proposed spectrophotometric methods showed a higher greenness score than the reported technique according to the Analytical Eco-Scale and the GAPI approaches.

Compatibility between materials was studied using DSC (Fig. 1) where the presence of the peaks of the studied drugs suggested the absence of interaction and hence compatibility between the drugs and PVA.

The combined and individual effect of the formulation variables on the selected responses was studied using Design-Expert software. Developed formulations had adequate TS (Table 2) indicating sufficient strength for the formulated dressing [12]. Sufficient mechanical strength is required for wound dressing to support cellular healing processes and to ensure optimum physical protection of the wound [28]. TS was affected by PVA and PG concentrations and the number of FT cycles. PVA concentration had a positive effect on TS as higher TS was obtained by increasing PVA from 3 to 8%. Dressings with lower PVA values could have a loose polymer network leading to lower TS values. Similar results were observed in several previous studies [45, 46]. However, PG had an antagonistic effect on TS. Lower TS values were obtained by higher PG concentrations due to its plasticizing effect. PG molecules get inserted between polymer strands, breaking polymer–polymer interactions and elevating the molecular mobility of polymer strands which leads to decreased dressing stiffness [25]. For crosslinking, repeated FT cycles had a positive effect on TS due to the formation of newly ordered tightly combined microstructures by refreezing the PVA solution. These structures wouldn't longer be separated [47, 48].

Wound dressings need to be flexible, soft and elastic to adapt to different body parts. %EB values for developed dressings (Table 2) were in the acceptable range (35–120%) [12]. PVA had a mild positive effect on %EB. PG also had a positive impact where increased PG concentration resulted in a marked increase in %EB. This could be explained by the PG plasticizing effect which would increase dressing mobility and reduce its brittleness [49]. For crosslinking, increased crosslinking by repeated FT cycles produced a slight decrease in % EB.

Drugs released from formulations (Table 2 and Fig. 5) were assessed to ensure drug flux through the skin [50]. PVA exerted a negative effect on drugs' release where higher PVA concentration resulted in slower drug release. Higher PVA (matrix-forming polymer) concentrations resulted in more dense structures with subsequent sustained release patterns [10]. Alternately, PG concentration positively affected LV and RVS release

since the plasticizing action of PG increased intermolecular distance between polymer chains which favors water diffusion throughout the dressing [51]. Crosslinking showed a negative effect as it is believed to hamper water penetration into the dressing which renders drug release more sustained. The gelled layer formed by dressing contact with the dissolution medium controls water penetration and forms a barrier that controls drugs release [27].

Formulated dressings had acceptable weight. pH values (6.2 ± 0.25–6.7 ± 0.14) indicate the absence of any irritant effect on the applied skin (Table 5). Drug content confirmed uniform drug distribution in the prepared dressings, while folding endurance values indicated the dressing's ability to maintain their integrity during handling and application [46]. The swelling study showed higher swelling indices with higher PVA and PG levels (Table 5 and Supplementary Fig. 4). PG increased water absorption by increasing the mobility of polymer strands which exposes more of polymer chains for moisture sorption [51]. WVTR represents a critical physical property for wound dressing as very high WVTR could lead to wound dehydration, while very low WVTR results in the accumulation of exudates with increased risk of bacterial contamination and delayed healing. WVTR values between 2000 and 2600 g/m^2/day (Table 5) could be suitable for wound dressing application [43, 52, 53]. PG increases WVTR by promoting intermolecular distance which favors water diffusion throughout the dressing [54]. On the contrary, higher PVA concentration decreased WVTR by the increased gelling property with subsequent narrow pores/channels responsible for vapor transmission [29].

In order to achieve a controlled release for 24 h, optimum values for LV and RVS release at 12th h were set to 50%. TS and %EB values were maximized to ensure dressing durability and flexibility in the applied area. Optimized formulation was prepared, and experimental values were compared to predicted ones. No major variations between observed and predicted responses (percentage error < 10%) assured the validity of the developed equations and their predictability within the context of data uncertainty.

Daily application of the developed dressings did not induce any inflammatory responses or produce any observed erythema. This indicates the biocompatibility of applied dressings. Time-dependent progression in wound contraction percent was observed in tested groups (Fig. 6a and b). Higher contraction percentage in the group treated with RVS/LV dressing compared to other groups confirmed the high and synergistic wound healing ability of both drugs. Results indicate that RVS potentiates the healing capability of LV. This can be related to its stimulation of endothelial cells and microvascular production along with inhibition of wound healing inhibitors [33, 55]. Wound healing was further confirmed by histopathological examination. Wound healing efficacy can be identified by re-epithelialization which is necessary for wound closure. Granulation tissue (GT) is formed on the wound surface as a newly constructed skin layer during the healing process. It consists of connective tissues and tiny blood vessels and is known for its ability to fill wounds. Hence, the presence of newly formed epithelium, along with granulation thickness represents positive signs for the healing process. Lower degrees of inflammation and congestion and the appearance of granulation tissue in animals treated with RVS/LV dressings confirm successful re-epithelialization. Compared to other groups, optimized formulation with drug combination had reduced congestion and inflammation. These signs indicate a complete and fast wound healing process by such formulation. Combined LV and RVS dressing showed the ability to induce almost complete tissue regeneration and optimum wound healing suggesting the use of these drugs in topical wound healing platforms [31, 32].

Conclusions

A novel formulation of a wound dressing combining LV and RVS was developed. The formulation underwent optimization to achieve a wound dressing that possesses satisfactory mechanical strength, flexibility and appropriate release for both prescribed medications. The results demonstrated that the optimized formulation exhibited superior wound healing capabilities, characterized by increased wound contraction, reduced inflammatory infiltration and optimal epithelialization, in comparison to dressings containing LV or RVS. The results of the study provide evidence in favor of employing this innovative combination in the context of wound healing applications. It is important to highlight that developing an environmentally friendly and cost-effective analytical technique capable of concurrently quantifying (LV) and (RVS) was achieved. Three spectrophotometric approaches, namely derivative of ratio spectrophotometry, first derivative and mean centering, were devised for the simultaneous quantification of RVS and LV in both the new formulation and pure form. An assessment of their environmental sustainability was conducted using the Analytical Eco-Scale and the Green Analytical Procedure Index (GAPI) indicating their minimal environmental impact.

Abbreviations

RVS	Rosuvastatin calcium
LV	Levofloxacin
PVA	Polyvinyl alcohol
TS	Tensile strength

EB	Elongation to break
PG	Propylene glycol
FT	Freeze–thaw
GAPI	Green Analytical Procedure Index
WVTR	Water vapor transmission rate
SI	Swelling index

Supplementary Information

The online version contains supplementary material available at https://doi.org/10.1186/s43094-024-00698-y.

Additional file 1.

Acknowledgements
Not applicable.

Author contributions
All authors contributed to the study conception and design. Experiment and data collection were performed by MAA, AOE, IAK, SEA and OAA. Data analysis and interpretation were performed by MAA, AOE, HAE, KHAM and AHE. The first draft of the manuscript was written by MAA, AOE, IAK, SEA, OAA, HAE, KHAM and AHE. Final manuscript was revised by MAA, IAK and HAE. All authors read and approved the final manuscript.

Funding
No funding.

Availability of data and materials
All data generated or analyzed during this study are included in this published article and its supplementary information files.

Declarations

Ethics approval and consent to participate
Animal study was conducted in accordance with the ethics committee, Faculty of Pharmacy (Girls), Al-Azhar University, Egypt (NUB-410–23).

Consent for publication
Not applicable.

Competing interests
The authors declare that they have no competing interests.

Author details
[1]Department of Pharmaceutics and Pharmaceutical Technology, Faculty of Pharmacy (Girls), Al-Azhar University, Cairo 11884, Egypt. [2]Analytical Chemistry Department, Faculty of Pharmacy (Girls), Al-Azhar University, Cairo 11884, Egypt. [3]Department of Pharmaceutical Sciences, School of Pharmacy and Physician Assistant Studies, University of Saint Joseph, West Hartford, CT 06117, USA.

Received: 5 July 2024 Accepted: 2 September 2024
Published online: 23 September 2024

References

1. Farghaly Aly U, Abou-Taleb HA, Abdellatif AA, Sameh Tolba N (2019) Formulation and evaluation of simvastatin polymeric nanoparticles loaded in hydrogel for optimum wound healing purpose. Drug Des Dev Ther 13:1567–1580. https://doi.org/10.2147/DDDT.S198413
2. Thapa RK, Diep DB, Tønnesen HH (2020) Topical antimicrobial peptide formulations for wound healing: current developments and future prospects. Acta Biomater 103:52–67. https://doi.org/10.1016/j.actbio.2019.12.025
3. Clark LA, Adams S, Bezwada P, O'Brien T, Schultz G (2003) The effect of levofloxacin on wound healing in rabbit and monkey models. Investig Ophthalmol Vis Sci 44:3845–3845
4. Valizadeh A, Shirzad M, Pourmand MR, Farahmandfar M, Sereshti H, Amani A (2021) Levofloxacin nanoemulsion gel has a powerful healing effect on infected wound in streptozotocin-induced diabetic rats. Drug Deliv Transl Res 11:292–304. https://doi.org/10.1007/s13346-020-00794-5
5. Farsaei S, Khalili H, Farboud ES (2012) Potential role of statins on wound healing: review of the literature. Int Wound J 9:238–247. https://doi.org/10.1111/j.1742-481X.2011.00888.x
6. Zaki RM, Seshadri VD, Mutayran AS, Elsawaf LA, Hamad AM, Almurshedi AS, Yusif RM, Said M (2022) Wound healing efficacy of rosuvastatin transethosomal gel, I optimal optimization, histological and in vivo evaluation. Pharmaceutics 14:2521. https://doi.org/10.3390/pharmaceutics14112521
7. Al-Kuraishy HM, Al-Gareeb AI, Al-Buhadily AK (2018) Rosuvastatin as forthcoming antibiotic or as adjuvant additive agent: in vitro novel antibacterial study. J Lab Phys 10:271–275. https://doi.org/10.4103/JLPJLP_170_17
8. Abdelaziz AA, El-Barrawy MA, El-Nagar RAM (2021) Potent synergistic combination of rosuvastatin and levofloxacin against Staphylococcus aureus: in vitro and in vivo study. J Appl Microbiol 131:182–196. https://doi.org/10.1111/jam.14968
9. Negut I, Grumezescu V, Grumezescu AM (2018) Treatment strategies for infected wounds. Molecules 23:2392. https://doi.org/10.3390/molecules23092392
10. Górska A, Krupa A, Majda D, Kulinowski P, Kurek M, Węglarz WP, Jachowicz R (2021) Poly(vinyl alcohol) cryogel membranes loaded with resveratrol as potential active wound dressings. AAPS PharmSciTech 22:109–109. https://doi.org/10.1208/s12249-021-01976-1
11. Ramnath V, Sekar S, Sankar S, Sankaranarayanan C, Sastry TP (2012) Preparation and evaluation of biocomposites as wound dressing material. J Mater Sci Mater Med 23:3083–3095. https://doi.org/10.1007/s10856-012-4765-5
12. Basit HM, Ali M, Shah MM, Shah SU, Wahab A, Albarqi HA, Alqahtani AA, Walbi IA, Khan NR (2021) Microwave enabled physically cross linked sodium alginate and pectin film and their application in combination with modified chitosan-curcumin nanoparticles. A novel strategy for 2nd degree burns wound healing in animals. Polymers 13:2716. https://doi.org/10.3390/polym13162716
13. Gajra B, Pandya SS, Singh S, Rabari HA (2014) Mucoadhesive hydrogel films of econazole nitrate: formulation and optimization using factorial design. J Drug Deliv 2014:305863. https://doi.org/10.1155/2014/305863
14. Hwang M-R, Kim JO, Lee JH, Kim YI, Kim JH, Chang SW, Jin SG, Kim JA, Lyoo WS, Han SS, Ku SK, Yong CS, Choi H-G (2010) Gentamicin-loaded wound dressing with polyvinyl alcohol/dextran hydrogel: gel characterization and in vivo healing evaluation. AAPS PharmSciTech 11:1092–1103. https://doi.org/10.1208/s12249-010-9474-0
15. Gupta A, Mishra P, Shah K (2009) Simple UV spectrophotometric determination of rosuvastatin calcium in pure form and in pharmaceutical formulations. J Chem 6:89–92. https://doi.org/10.1155/2009/956712
16. Kassab NM, Amaral MS, Singh AK, Santoro M (2010) Development and validation of UV spectrophotometric method for determination of levofloxacin in pharmaceutical dosage forms. Quím Nova 33(4):968–971. https://doi.org/10.1590/S0100-40422010000400037
17. Qassim A (2015) Determination of levofloxacin in pharmaceutical formulationtavanic by visible spectrophotometry of its chelating complex with aluminum ion (III). Int J Dev Res 5(6):4702–4706
18. Egunova OR, Reshetnikova IS, Kazimirova KO, Shtykov SN (2020) Magnetic solid-phase extraction and fluorimetric determination of some fluoroquinolones. J Anal Chem 75:24–33. https://doi.org/10.1134/S1061934820010062
19. Yi W, Han C, Li Z, Guo Y, Liu M, Dong C (2021) A strategy of electrochemical simultaneous detection of acetaminophen and levofloxacin in water based on g-C3N4 nanosheet-doped graphene oxide. Environ Sci Nano 8:258–268. https://doi.org/10.1039/D0EN00858C
20. Caglar S, Toker S (2013) Determination of rosuvastatin at picogram level in serum by fluorimetric derivatization with 9-anthryldiazomethane using HPLC. J Chromatogr Sci 51:53–58. https://doi.org/10.1093/chromsci/bms105

21. Yıldırım S, Karakoç HN, Yaşar A, Köksal İ (2020) Determination of levofloxacin, ciprofloxacin, moxifloxacin and gemifloxacin in urine and plasma by HPLC–FLD–DAD using pentafluorophenyl core–shell column: application to drug monitoring. Biomed Chromatogr 34:e4925. https://doi.org/10.1002/bmc.4925
22. Abbas NS, Derayea SM, Omar MA, Saleh GA (2020) TLC-spectrodensitometric method for simultaneous determination of dapagliflozin and rosuvastatin in rabbit plasma: stability indicating assay and kinetic studies. RSC Adv 10:40795–40805. https://doi.org/10.1039/D0RA05628F
23. Zheng X, Jongedijk EM, Hu Y, Kuhlin J, Zheng R, Niward K, Paues J, Xu B, Davies Forsman L, Schön T, Bruchfeld J, Alffenaar J-WC (2020) Development and validation of a simple LC-MS/MS method for simultaneous determination of moxifloxacin, levofloxacin, prothionamide, pyrazinamide and ethambutol in human plasma. J Chromatogr B 1158:122397. https://doi.org/10.1016/j.jchromb.2020.122397
24. Panda J, Rao MEB, Swain S, Patra CN, Jena BR (2022) Formulation development, optimization and characterization of mucoadhesive minitablets of cefuroxime axetil: in vitro, ex vivo and in vivo pharmacokinetic evaluation. Beni-Suef Univ J Basic Appl Sci 11:123. https://doi.org/10.1186/s43088-022-00303-2
25. ElMeshad AN, El Hagrasy AS (2011) Characterization and optimization of orodispersible mosapride film formulations. AAPS PharmSciTech 12:1384–1392. https://doi.org/10.1208/s12249-011-9713-z
26. Hoseinpour Najar M, Minaiyan M, Taheri A (2018) Preparation and in vivo evaluation of a novel gel-based wound dressing using arginine–alginate surface-modified chitosan nanofibers. J Biomater Appl 32:689–701. https://doi.org/10.1177/0885328217739562
27. Zarandona I, Minh NC, Trung TS, de la Caba K, Guerrero P (2021) Evaluation of bioactive release kinetics from crosslinked chitosan films with Aloe vera. Int J Biol Macromol 182:1331–1338. https://doi.org/10.1016/j.ijbiomac.2021.05.087
28. Tenorová K, Masteiková R, Pavloková S, Kostelanská K, Bernatonienė J, Vetchý D (2022) Formulation and evaluation of novel film wound dressing based on collagen/microfibrillated carboxymethylcellulose blend. Pharmaceutics 14:782. https://doi.org/10.3390/pharmaceutics14040782
29. Kaur R, Sharma A, Puri V, Singh I (2019) Preparation and characterization of biocomposite films of carrageenan/locust bean gum/montmorrillonite for transdermal delivery of curcumin. Bioimpacts 9:37–43. https://doi.org/10.15171/bi.2019.05
30. Nada AA, Arul MR, Ramos DM, Kroneková Z, Mosnáček J, Rudraiah S, Kumbar SG (2018) Bioactive polymeric formulations for wound healing. Polym Adv Technol 29:1815–1825. https://doi.org/10.1002/pat.4288
31. Salem HF, Nafady MM, Ewees MGE-D, Hassan H, Khallaf RA (2022) Rosuvastatin calcium-based novel nanocubic vesicles capped with silver nanoparticles-loaded hydrogel for wound healing management: optimization employing Box–Behnken design: in vitro and in vivo assessment. J Liposome Res 32:45–61. https://doi.org/10.1080/08982104.2020.1867166
32. Ahmed LM, Hassanein KMA, Mohamed FA, Elfaham TH (2023) Formulation and evaluation of simvastatin cubosomal nanoparticles for assessing its wound healing effect. Sci Rep 13:17941. https://doi.org/10.1038/s41598-023-44304-2
33. Gomaa SF, Madkour TM, Moghannem S, El-Sherbiny IM (2017) New polylactic acid/ cellulose acetate-based antimicrobial interactive single dose nanofibrous wound dressing mats. Int J Biol Macromol 105:1148–1160. https://doi.org/10.1016/j.ijbiomac.2017.07.145
34. Bansal M, Mittal N, Yadav SK, Khan G, Gupta P, Mishra B, Nath G (2018) Periodontal thermoresponsive, mucoadhesive dual antimicrobial loaded in-situ gel for the treatment of periodontal disease: preparation, in-vitro characterization and antimicrobial study. J Oral Biol Craniofacial Res 8:126–133. https://doi.org/10.1016/j.jobcr.2017.12.005
35. Inam S, Irfan M, Lali NU, Khalid Syed H, Asghar S, Khan IU, Khan SUD, Iqbal MS, Zaheer I, Khames A, Abou-Taleb HA, Abourehab MAS (2022) Development and characterization of Eudragit® EPO-based solid dispersion of rosuvastatin calcium to foresee the impact on solubility, dissolution and antihyperlipidemic activity. Pharmaceuticals 15:492. https://doi.org/10.3390/ph15040492
36. Verma R, Kaushik A, Almeer R, Rahman MH, Abdel-Daim MM, Kaushik D (2021) Improved pharmacodynamic potential of rosuvastatin by self-nanoemulsifying drug delivery system: an in vitro and in vivo evaluation. Int J Nanomed 16:905–924. https://doi.org/10.2147/IJN.S287665
37. Gupta B, Anjum S, Ikram S (2013) Characterization and physiochemical studies of crosslinked thiolated polyvinyl alcohol hydrogels. Polym Bull 70:2709–2725. https://doi.org/10.1007/s00289-013-0982-4
38. Salinas F, Nevado JJB, Mansilla AE (1990) A new spectrophotometric method for quantitative multicomponent analysis resolution of mixtures of salicylic and salicyluric acids. Talanta 37:347–351. https://doi.org/10.1016/0039-9140(90)80065-N
39. Abdel Razeq SA, El Demerdash AO, Fouad MM, El Sanabary HF (2019) Densitometric and ratio spectra methods for simultaneous determination of sulfaquinoxaline sodium and pyrimethamine in binary mixture. Bull Fac Pharm Cairo Univ 57:35–45. https://doi.org/10.21608/bfpc.2019.7290.1002
40. Shi M, Zheng X, Zhang N, Guo Y, Liu M, Yin L (2023) Overview of sixteen green analytical chemistry metrics for evaluation of the greenness of analytical methods. TrAC Trends Anal Chem 166:117211. https://doi.org/10.1016/j.trac.2023.117211
41. Yabré M, Ferey L, Somé TI, Sivadier G, Gaudin K (2020) Development of a green HPLC method for the analysis of artesunate and amodiaquine impurities using Quality by Design. J Pharm Biomed Anal 190:113507. https://doi.org/10.1016/j.jpba.2020.113507
42. Ibrahim AE, Saleh H, Elhenawee M (2019) Assessment and validation of green stability indicating RP-HPLC method for simultaneous determination of timolol and latanoprost in pharmaceutical dosage forms using eco-friendly chiral mobile phase. Microchem J 148:21–26. https://doi.org/10.1016/j.microc.2019.04.059
43. Delavari MM, Stiharu I (2022) Preparation and characterization of eco-friendly transparent antibacterial starch/polyvinyl alcohol materials for use as wound-dressing. Micromachines 13:960. https://doi.org/10.3390/mi13060960
44. Sood A, Granick MS, Tomaselli NL (2014) Wound dressings and comparative effectiveness data. Adv Wound Care 3:511–529
45. Chauhan S, Bansal M, Khan G, Yadav SK, Singh AK, Prakash P, Mishra B (2018) Development, optimization and evaluation of curcumin loaded biodegradable crosslinked gelatin film for the effective treatment of periodontitis. Drug Dev Ind Pharm 44:1212–1221. https://doi.org/10.1080/03639045.2018.1439501
46. Parhi R, Suresh P (2016) Formulation optimization and characterization of transdermal film of simvastatin by response surface methodology. Mater Sci Eng C 58:331–341. https://doi.org/10.1016/j.msec.2015.08.056
47. Ahmed AS, Mandal UK, Taher M, Susanti D, Jaffri JM (2018) PVA-PEG physically cross-linked hydrogel film as a wound dressing: experimental design and optimization. Pharm Dev Technol 23:751–760. https://doi.org/10.1080/10837450.2017.1295067
48. Li C, Zhang Y, Han Y, Zhao X, Tian F (2021) Freeze–thaw enhanced stability and mechanical strength of polysaccharide-based sodium alginate/hyaluronic acid films. J Food Saf 42:e12958. https://doi.org/10.1111/jfs.12958
49. Mazumder S, Pavurala N, Manda P, Xu X, Cruz CN, Krishnaiah YSR (2017) Quality by Design approach for studying the impact of formulation and process variables on product quality of oral disintegrating films. Int J Pharm 527:151–160. https://doi.org/10.1016/j.ijpharm.2017.05.048
50. Patel RP, Gaiakwad DR, Patel NA (2014) Formulation, optimization, and evaluation of a transdermal patch of heparin sodium. Drug Discov Ther 8:185–193. https://doi.org/10.5582/ddt.2014.01030
51. Joshi R, Garud N (2021) Development, optimization and characterization of flurbiprofen matrix transdermal drug delivery system using Box–Behnken statistical design. Future J Pharm Sci 7:57. https://doi.org/10.1186/s43094-021-00199-2
52. Nuutila K, Eriksson E (2021) Moist wound healing with commonly available dressings. Adv Wound Care 10:685–698. https://doi.org/10.1089/wound.2020.1232
53. Xu R, Xia H, He W, Li Z, Zhao J, Liu B, Wang Y, Lei Q, Kong Y, Bai Y, Yao Z, Yan R, Li H, Zhan R, Yang S, Luo G, Wu J (2016) Controlled water vapor transmission rate promotes wound-healing via wound re-epithelialization and contraction enhancement. Sci Rep 6:24596. https://doi.org/10.1038/srep24596

54. Nešić A, Onjia A, Davidović S, Dimitrijević S, Errico ME, Santagata G, Malinconico M (2017) Design of pectin-sodium alginate based films for potential healthcare application: study of chemico-physical interactions between the components of films and assessment of their antimicrobial activity. Carbohydr Polym 157:981–990. https://doi.org/10.1016/j.carbpol.2016.10.054
55. Mao G, Tian S, Shi Y, Yang J, Li H, Tang H, Yang W (2023) Preparation and evaluation of a novel alginate-arginine-zinc ion hydrogel film for skin wound healing. Carbohydr Polym 311:120757. https://doi.org/10.1016/j.carbpol.2023.120757

Publisher's Note